

# Heterogeneous- $k$ -core versus Bootstrap Percolation on Complex Networks

G. J. Baxter,<sup>1,\*</sup> S. N. Dorogovtsev,<sup>1,2</sup> A. V. Goltsev,<sup>1,2</sup> and J. F. F. Mendes<sup>1</sup>

<sup>1</sup>*Departamento de Física, I3N, Universidade de Aveiro,  
Campus Universitário de Santiago, 3810-193 Aveiro, Portugal*

<sup>2</sup>*A. F. Ioffe Physico-Technical Institute, 194021 St. Petersburg, Russia*

(Dated: February 16, 2022)

We introduce the heterogeneous- $k$ -core, which generalizes the  $k$ -core, and contrast it with bootstrap percolation. Vertices have a threshold  $k_i$  which may be different at each vertex. If a vertex has less than  $k_i$  neighbors it is pruned from the network. The heterogeneous- $k$ -core is the sub-graph remaining after no further vertices can be pruned. If the thresholds  $k_i$  are 1 with probability  $f$  or  $k \geq 3$  with probability  $(1 - f)$ , the process forms one branch of an activation-pruning process which demonstrates hysteresis. The other branch is formed by ordinary bootstrap percolation. We show that there are two types of transitions in this heterogeneous- $k$ -core process: the giant heterogeneous- $k$ -core may appear with a continuous transition and there may be a second, discontinuous, hybrid transition. We compare critical phenomena, critical clusters and avalanches at the heterogeneous- $k$ -core and bootstrap percolation transitions. We also show that network structure has a crucial effect on these processes, with the giant heterogeneous- $k$ -core appearing immediately at a finite value for any  $f > 0$  when the degree distribution tends to a power law  $P(q) \sim q^{-\gamma}$  with  $\gamma < 3$ .

PACS numbers: 64.60.aq, 64.60.ah, 05.10.-a, 05.70.Fh

Bootstrap percolation and the  $k$ -core are closely related concepts, and in fact it is easy to confuse the two. Both belong to a new class of systems with hybrid phase transitions, yet it can be clearly shown that the two processes do not map onto each other. Here we elucidate the relationship and differences between these two concepts by introducing a generalization of the  $k$ -core, the heterogeneous- $k$ -core.

The  $k$ -core is the maximal sub-graph whose vertices all have internal degree at least  $k$  [1]. It has proved a useful tool giving insight into the deep structure of complex networks [2–6], and has found applications in diverse areas, from rigidity [7] and jamming [8] transitions to real neural networks [9, 10] and evolution [11]. The  $k$ -core has been extensively studied on tree-like networks, starting with Bethe lattices [12, 13] and Random graphs [14–16], before finally being extended to arbitrary degree distributions [5, 17–19]. Hyperbolic lattices have also been considered [20]. Other studies, mostly numerical, have considered the sizes of culling avalanches [21–23]. Results on non tree-like graphs have been largely numerical [24, 25], although some analytic results incorporating clustering have recently been obtained [26, 27]. At the same time, bootstrap percolation has emerged as a useful model for a variety of applications such as neuronal activity [28–30], jamming and rigidity transitions and glassy dynamics [31, 32], and magnetic systems [33]. In bootstrap percolation, a set of seed vertices is initially activated, and other vertices become active if they have  $k$  active neighbors. This process has been investigated on two and three dimensional lattices (see [34–37] and references therein). Bootstrap percolation has been studied

on the random regular graph [38, 39], on infinite trees [40], and most recently general complex networks [41]. Finite random graphs have also been studied [42]. An interesting alternative formulation is the Watts model of opinions, in which the threshold is defined as a certain fraction of the neighbors rather than an absolute number [43]. These processes may also be generalized so that the thresholds may be different at each vertex [41, 44].

Here we introduce a generalization of the  $k$ -core, the heterogeneous- $k$ -core. In the heterogeneous- $k$ -core, each vertex  $i$  in a network has a hidden variable, its threshold value  $k_i$ . The heterogeneous- $k$ -core is the largest sub-graph whose members have at least as many neighbors as their threshold value  $k_i$ . This may include finite clusters as well as any giant component. If the  $k_i$  are all equal we recover the standard  $k$ -core. We define a simple representative example of the heterogeneous- $k$ -core (HKC) in which vertices have a threshold of either 1 or  $k \geq 3$ , distributed randomly through the network with probabilities  $f$  and  $(1 - f)$  respectively. This can be directly contrasted with bootstrap percolation (BPC), in which vertices can be of two types: with probability  $f$  they are ‘seed’ vertices which are always active, while with probability  $(1 - f)$  vertices become active only if their number of active neighbors reaches a threshold  $k$ . The difference between these two processes arises because bootstrap percolation is an activation process, beginning from a sparsely activated network, while the heterogeneous- $k$ -core is a pruning process [14, 15], beginning from a complete graph. It is thus possible to think of these two processes as two branches of a hysteresis loop in an activation-pruning process.

We observe two transitions in the size of the giant heterogeneous- $k$ -core (giant-HKC): a continuous transition similar to that found in ordinary percolation, and a discontinuous, hybrid, transition, similar to that found

---

\*gjbaxter@ua.pt

for the ordinary  $k$ -core. We find a complex phase diagram for this giant-HKC with respect to the proportion of each threshold and the amount of damage to the network, in which, depending on the parameter region, either transition may occur first. Two similar transitions are observed in the phase diagram of the giant component of active vertices in bootstrap percolation (giant-BPC).

Finally, we show that network heterogeneity plays an important role. When the second moment of the degree distribution is finite but the third moment diverges, the giant-HKC (or giant-BPC) appears at a finite threshold but not linearly, instead being a higher order transition. When the second moment of the degree distribution diverges – as in scale-free networks – the thresholds may disappear completely, so that the giant-HKC (or giant-BPC) appears discontinuously at a finite value for any  $f > 0$  or  $p > 0$ .

### I. THE HETEROGENEOUS- $k$ -CORE AND BOOTSTRAP PERCOLATION

Consider an arbitrary, uncorrelated, sparse complex network, defined by its degree distribution  $P(q)$ . In the infinite size limit, such networks are locally tree-like, a property which enables the analysis we will use. The network may be damaged to some extent by the removal of vertices uniformly at random. The fraction of surviving vertices is  $p$ .

In the heterogeneous- $k$ -core, each vertex of a network is assigned a variable  $k_i \in \{0, 1, 2, \dots\}$ . The  $k_i$  values are assumed to be uncorrelated, selected from a distribution  $Q_k(r)$ . The heterogeneous- $k$ -core is then the largest subgraph of the network for which each vertex  $i$  has at least  $k_i$  neighbors within the heterogeneous- $k$ -core. To find the heterogeneous- $k$ -core of a given network, we start with the full network, and prune any vertices whose degree is less than its value of  $k_i$ . As a result of this pruning, other vertices will lose neighbors, and may thus drop below their threshold, so we repeat the pruning until a stationary state is reached. The remaining sub-graph is the heterogeneous- $k$ -core. If it occupies a non-vanishing fraction of the original network in the limit that the size of the network goes to infinity, we say it is a giant heterogeneous- $k$ -core (giant-HKC).

If all  $k_i = 1$ , then the HKC is simply the connected component of the network, and the giant-HKC is the giant connected component, exactly as in ordinary percolation. As is well known [6, 45, 46] this appears with a continuous transition at the critical point  $p_c = \langle q \rangle / [\langle q^2 \rangle - \langle q \rangle]$ , where  $\langle q^n \rangle = \sum_i q^n P(q)$ . If  $k = 2$ , we again have a continuous transition, similar to ordinary percolation. If all  $k_i$  are equal to  $k \geq 3$ , then we have the ordinary  $k$ -core. In this case the giant  $k$ -core appears with a discontinuous hybrid transition [5, 8, 17, 47].

Let us briefly discuss the nature of hybrid phase transitions. These transitions form a specific new kind of

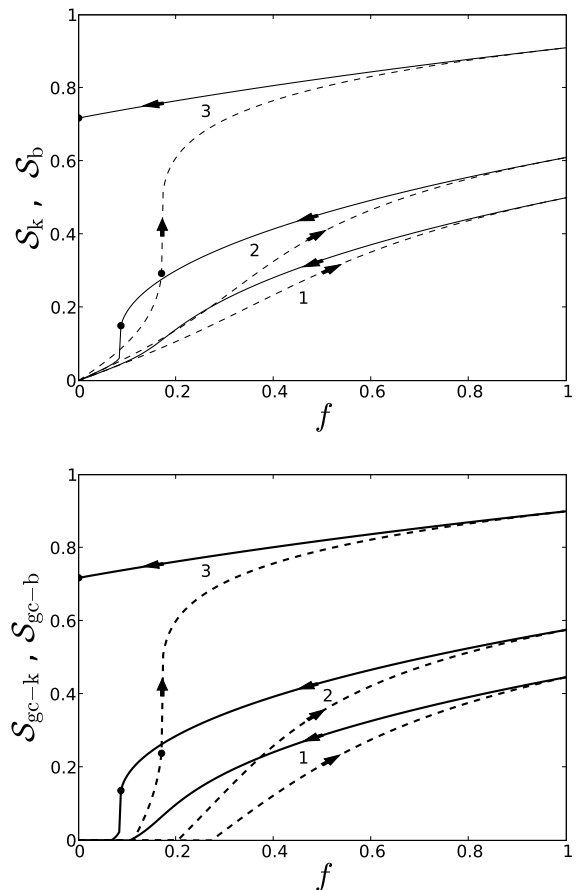


FIG. 1: Top: relative size  $S_k$  of the heterogeneous- $k$ -core (solid curves), which is the subgraph including all vertices which meet the threshold requirements of Eq. (1), and fraction  $S_b$  of active vertices in bootstrap percolation (dashed curves) as a function of  $f$  for the same network – an Erdős-Rényi graph of mean degree 5 – with the same  $k = 3$ , at three different values of  $p$ , corresponding to different regions of the phase diagrams Fig. 2. 1)  $p = 0.5$ , which is between  $p_c$  and  $p_s$  for both models. 2)  $p = 0.61$ , which is above  $p_{s-k}$  but still below  $p_{s-b}$ . 3)  $p = 0.91$ , which is above  $p_{f-k}$  and  $p_{s-b}$ . Each numbered pair forms the two branches of a hysteresis process, followed in the direction marked by the arrows. Bottom: Size  $S_{gc-k}$  of the giant heterogeneous- $k$ -core (solid) and size  $S_{gc-b}$  of the giant-BPC (dashed) as a function of  $f$  for the same network and the same values of  $p$ .

phase transition which combines a discontinuity like a first order phase transition with a critical singularity like a continuous phase transition. In thermodynamics, where the changes of a control parameter (e.g., decreasing/increasing temperature) are assumed to be infinitely slow, a first order transition has no hysteresis. In reality, the changes always occur with a small but finite rate, and the ‘heating’ and ‘cooling’ branches of a first order transition do not coincide, which indicates the presence of a metastable state and hysteresis. The width of the hysteresis increases with this rate until

some limit, which corresponds to the limiting metastable state. The resulting limiting curve for the order parameter has a square-root singularity at the breakdown point. For example, if we heat a ferromagnet with a first order phase transition sufficiently rapidly, the curve ‘magnetization  $M$  versus temperature  $T$ ’ has a singularity  $M(T) - M(T_b - 0) \propto \sqrt{T_b - T}$  at the breakdown point  $T_b$  and discontinuity, that is  $M(T_b - 0) > M(T_b + 0) = 0$ . After the breakdown, there is no singularity. The susceptibility also shows a singularity  $\chi(T < T_b) \propto 1/\sqrt{T_b - T}$  and has no singularity above  $T_b$ . In this sense, the hybrid (mixed) transition is a limiting metastable state for a first order phase transition. The important property is that the transition is asymmetrical. There are critical fluctuations and a divergent correlation length on only one side of the critical point. Continuous phase transitions demonstrate critical fluctuations and divergent correlation length on both sides of the transition. In first order phase transitions there are no critical fluctuations and correlation length is finite everywhere, including at the critical point.

In general we might expect a combination of continuous and hybrid transitions. To this end we first consider the simple case in which the  $k_i$  are distributed between two values, controlled by a parameter  $f$ . Specifically:

$$Q_k(r) = \begin{cases} f & \text{if } r = 1, \\ 1 - f & \text{if } r = k, \\ 0 & \text{otherwise,} \end{cases} \quad (1)$$

for some integer  $k \geq 3$ . This parameterized HKC has as its two limits ordinary percolation ( $f = 1$ ) and the original  $k$ -core ( $f = 0$ ).

We now contrast this model with bootstrap percolation. In bootstrap percolation, with probability  $f$ , a vertex is a ‘seed’ and is initially active, and remains active. The remaining vertices (a fraction  $1 - f$ ) become active if their number of active neighbors reaches or exceeds a threshold value  $k$ . Once activated, a vertex remains active. The activation of vertices may mean that new vertices now meet the threshold criterion, and hence become active. This activation process continues iteratively until a stationary state is reached. The seed and activated vertices in bootstrap percolation are analogous to the threshold 1 and threshold  $k$  groups in the heterogeneous- $k$ -core. We might expect then that the subgraph formed by the active vertices in the stationary state of bootstrap percolation might be related to the heterogeneous- $k$ -core. In fact, the two subgraphs are necessarily different, as we will describe in detail in Sec. II. Nevertheless, the two processes have some similar or analogous critical behaviors. Note that we are using a lower threshold of 1 for the generalized  $k$ -core, meaning isolated vertices are not counted as part of the HKC. We could also use a lower threshold of 0, which would include more vertices in the HKC, but would yield an identical giant-HKC. For this reason, we can compare with bootstrap percolation, in which the seed vertices have effectively a threshold of 0.

Because bootstrap percolation is an activation process, while the heterogeneous- $k$ -core is found by pruning, we can characterize them as two branches of the same process, with the difference between the curves shown in Fig. 1 indicating hysteresis. Consider beginning from a completely inactive network (that may be damaged so that some fraction  $p$  of vertices remain). As we gradually increase  $f$  from zero, under the bootstrap percolation process, more and more vertices become active (always reaching equilibrium before further increases of  $f$ ) until at a certain threshold value,  $f_{c1-b}$  a giant active component appears. As we increase  $f$  further, the size of the giant-BPC traces the dashed curves shown in Fig. 1. See also [41]. The direction of this process is indicated by the arrows on these curves. Finally at  $f = 1$  all undamaged vertices are active. Now we reverse the process, beginning with a fully active network, and gradually reducing  $f$ , de-activating (equivalent to pruning) vertices that fall below their threshold  $k_i$  under the heterogeneous- $k$ -core process. As  $f$  decreases, the solid curves in Fig. 1 will be followed, in the direction indicated by the arrows. Notice that the size of the giant-HKC for given values of  $f$  and  $p$  is always larger than the giant-BPC. The explanation for this difference will be explored in the following Section.

Let  $\mathcal{S}_k$  be the fraction of vertices that are in the heterogeneous- $k$ -core. That is, the total of all components, whether finite or infinite, that meet the threshold conditions. This is equal to the probability that an arbitrarily chosen vertex of the original network is in the heterogeneous- $k$ -core. Let  $\mathcal{S}_{gc-k}$  be the relative size of the giant heterogeneous- $k$ -core (that is, the subset of the heterogeneous- $k$ -core which forms a giant component) – also the probability that an arbitrarily chosen vertex is in the giant heterogeneous- $k$ -core. The fraction of vertices forming finite clusters is therefore  $\mathcal{S}_k - \mathcal{S}_{gc-k}$ . Note that in the standard  $k$ -core this is negligibly small. Similarly, let  $\mathcal{S}_b$  be the fraction of active vertices in the bootstrap percolation model, and  $\mathcal{S}_{gc-b}$  be the size of the giant component of active vertices. We construct self-consistency equations for  $\mathcal{S}_k$  and  $\mathcal{S}_{gc-k}$  in Appendix A. In networks without heavy-tailed degree distributions, that is, whose second moments do not diverge in the infinite size limit, we find two different transitions for each process.

We first briefly describe the transitions observed in bootstrap percolation, before comparing these with those found in the new heterogeneous- $k$ -core process. For bootstrap percolation, above a certain value of  $p$ , the giant active component (giant-BPC) may appear continuously from zero at a finite value of  $f$ ,  $f_{c1-b}$ , and grow smoothly with  $f$ , see the dashed lines 1 and 2 in the top panel of Fig. 1. For larger  $p$ , after the giant active component appears, there may also be a second discontinuous hybrid phase transition, at  $f_{c2-b}$ , as seen in the dashed line 3 of Fig. 1. There is a jump in the size of the giant active component  $\mathcal{S}_{gc-b}$  from the value at the critical point (marked by a circle on dashed line 3). When approaching

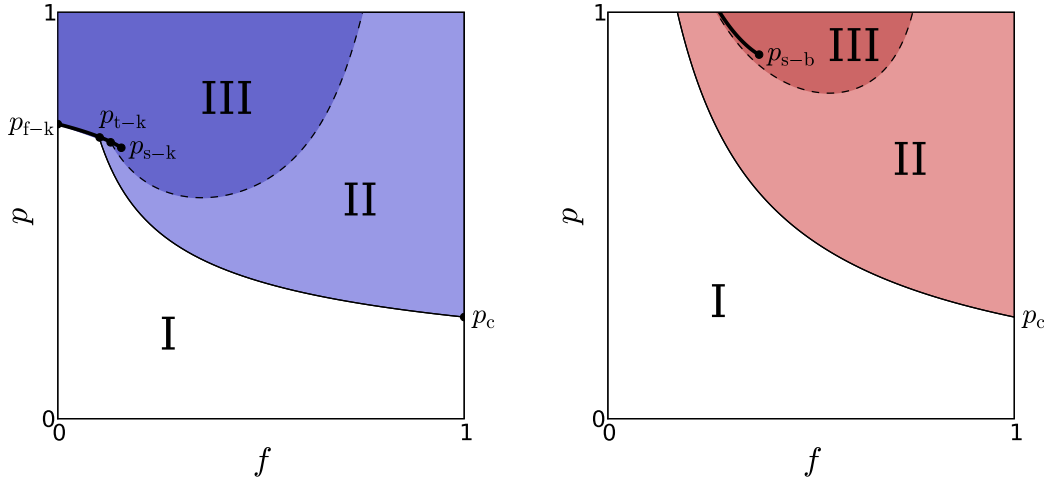


FIG. 2: Left: Phase diagrams for heterogeneous- $k$ -core (left) in the  $f$ - $p$  plane. The giant-HKC is present in regions II and III, appearing continuously at the threshold marked by the thin black curve. The hybrid, discontinuous transition occurs at the points marked by the heavy black line, beginning from  $p_{s-k}$ . Above  $p_{t-k}$  the first appearance of the giant-HKC is with a discontinuous transition. Above  $p_{f-k}$  the giant-HKC appears discontinuously for any  $f > 0$ . In region III the vertices with threshold  $k$  in the HKC form a giant connected component, which appears with a continuous transition (dashed curve). Right: Phase diagram for bootstrap percolation. The giant-BPC is present in regions II and III. The continuous appearance of the giant-BPC is marked by the thin solid curve, and the hybrid transition (beginning at  $p_{s-b}$ ) by a heavy solid curve. In region III the active vertices with threshold  $k$  form a giant connected component. These diagrams are for a Bethe lattice with degree 5, and for  $k = 3$ , but the diagram for any network with finite second moment of the degree distribution will be qualitatively the same. Note that the locations of the continuous transitions from region I to II and from II to III for bootstrap percolation with  $k \rightarrow k - 1$  coincide (up to the point where the discontinuous transition is encountered) with those for the heterogeneous- $k$ -core. The special critical point  $p_{s-b}$  with  $k$  reduced by 1 also coincides with  $p_{s-k}$  (see also Appendix A).

from below, the difference of  $\mathcal{S}_{\text{gc-b}}$  from the critical value goes as the square root of the distance from the critical point:

$$\mathcal{S}_b(f) = \mathcal{S}_b(f_{c2-b}) - a(f_{c2-b} - f)^{1/2}. \quad (2)$$

See [41] for a complete description of the bootstrap percolation results.

For the heterogeneous- $k$ -core, we see a different but analogous pair of transitions. Again, for a given  $p$ , the giant heterogeneous- $k$ -core (giant-HKC) appears continuously from zero above some critical value of  $f$ ,  $f_{c1-k}$ . There may also be a second transition, at  $f_{c2-k}$ , where again we see a discontinuity in the size of the giant-HKC. Now however, the square root scaling occurs as the critical point is approached from above:

$$\mathcal{S}_k(f) = \mathcal{S}_k(f_{c2-k}) + a(f - f_{c2-k})^{1/2}. \quad (3)$$

See solid line 2 in Fig. 1. Another important difference is that, while for bootstrap percolation the discontinuous transition is always above the first appearance of the giant-BPC –  $f_{c2-b} > f_{c1-b}$ , but for the heterogeneous- $k$ -core,  $f_{c2-k}$  may be greater than  $f_{c1-k}$  – so that the first appearance of the giant-HKC is similar to that found in ordinary percolation – or less than  $f_{c1-k}$ , with the giant-HKC appearing discontinuously from zero, as in the ordinary  $k$ -core [8, 17, 47] (see Fig. 1).

The overall behavior with respect to the parameters  $p$  and  $f$  of each model is summarized by the phase diagrams in Fig. 2. The diagrams are qualitatively the same for any degree distribution with finite second moment. Considering first the heterogeneous- $k$ -core, a giant-HKC is absent in the region labelled I. For  $p$  below the percolation threshold  $p_c$ , the giant-HKC never appears for any  $f$ . Above  $p_c$ , the giant-HKC appears with a continuous transition, growing linearly with  $f$  (or  $p$  for that matter) close to the critical point. The threshold is indicated by the thin black line in the Figure, which divides regions I and II. Compare line 1 of Fig. 1. From  $p_{s-k}$  a second, discontinuous, hybrid transition appears. This is marked by the heavy black curve in Fig. 2. As already noted in Eq. (3) the size of the giant-HKC grows as the square root of the distance above this second critical point. At the special point  $p_{s-k}$ , however, the size of the discontinuity reduces to zero, and the scaling near the critical point is cube root:

$$\mathcal{S}_k(f) = \mathcal{S}_k(f_{c2-k}) + a(f - f_{c2-k})^{1/3}. \quad (4)$$

At first the hybrid transition occurs after the continuous appearance of the giant-HKC (see line 2 of Fig. 1), but at  $p_{t-k}$  the two transitions cross, and the giant-HKC begins to appear immediately with a jump. Finally at  $p_{f-k}$ , the giant-HKC begins to appear discontinuously immediately

from  $f = 0$  (line 3 of Fig. 1). Thus, the first appearance of the giant-HKC has a classical percolation like transition below  $p_{t-k}$ , while above  $p_{t-k}$  the appearance is similar to that found in the ordinary  $k$ -core. Within the heterogeneous- $k$ -core, the vertices with threshold  $k$  may form a giant component themselves. This occurs in the region labelled III. This giant component appears with a continuous transition.

For bootstrap percolation, the giant active component again appears only above the percolation threshold  $p_c$ . It also appears at first with a linear, continuous transition (when the degree distribution has finite third moment), but at a larger value of  $f$ . The point of appearance is marked by the thin curve in Fig. 2 which divides regions I and II. Again, a second transition appears for larger  $p$ , beginning at the special critical point  $p_{s-b}$ . This transition is marked by the heavy solid curve in the Figure. See also line 3 of Fig. 1. The scaling near the hybrid transition is again square root, but this time only when approaching the transition from below. At the special critical point  $p_{s-b}$ , the scaling becomes cube root:

$$\mathcal{S}_b(f) = \mathcal{S}_b(f_{c2-b}) - a(f_{c2-b} - f)^{1/3}. \quad (5)$$

Note the difference between Eqs. (2) and (3) and between (5) and (4). In bootstrap percolation, the hybrid transition always occurs above the continuous one, and neither reaches  $f = 0$ . Again, the active threshold  $k$  vertices form a giant component in Region III. Note also that the special critical point  $p_{s-b} > p_{f-k}$ , so that for a given  $p$  we may have a hybrid transition for the HKC or for BPC, but not for both. It turns out that the special critical point  $p_{s-b}$  for bootstrap percolation whose value of  $k$  is one less coincides with the special critical point for the heterogeneous- $k$ -core. Furthermore, the location of the continuous appearance of the giant heterogeneous- $k$ -core for a given  $k$  also coincides with the appearance of the giant component of bootstrap percolation for  $k - 1$ . The same is also true for the appearance of the giant components of vertices with threshold  $k$ . This is clear from the equations given in Appendix A. If the value of  $k$  is increased, the locations of the hybrid transitions move toward larger values of  $p$ , and there is a limiting value of  $k$  after which these transitions disappear altogether. For both the heterogeneous- $k$ -core and bootstrap percolation, this limit is proportional to the mean degree. Note also that the continuous transition also moves slightly with increasing  $k$ , and in the limit  $k \rightarrow \infty$ , tends to the line  $pf = p_c$  for both processes.

## II. SUBCRITICAL CLUSTERS, CORONA CLUSTERS, AVALANCHES

It is clear from Figs. 1 and 2 that even though bootstrap percolation and the heterogeneous- $k$ -core described above have the same thresholds and proportions of each kind of vertex, the equilibrium size of the respective giant components is very different. The difference results

from the top-down vs bottom-up ways in which they are constructed. To find the heterogeneous- $k$ -core, we begin with the full network, and prune vertices which don't meet the criteria, until we reach equilibrium. In contrast, bootstrap percolation begins with a largely inactive network, and successively activates vertices until equilibrium is reached. To see the effect of this difference, we now describe an important concept: the subcritical clusters of bootstrap percolation.

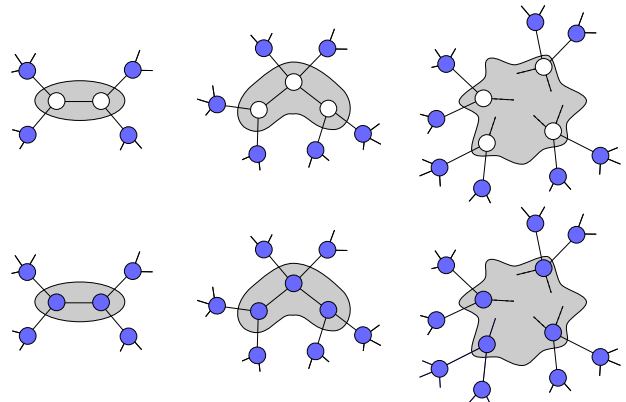


FIG. 3: Top row: Subcritical clusters of different sizes in bootstrap percolation. Left: Because they start in an inactive state, two connected vertices (shaded area) cannot become active if each has  $k - 1$  active neighbors. (In this example  $k = 3$ .) The same follows for clusters of three (center) or more vertices (right). If any member of a subcritical cluster gains another active neighbor, an avalanche of activations encompasses the whole cluster. Bottom row: Similar clusters would be included in the heterogeneous- $k$ -core.

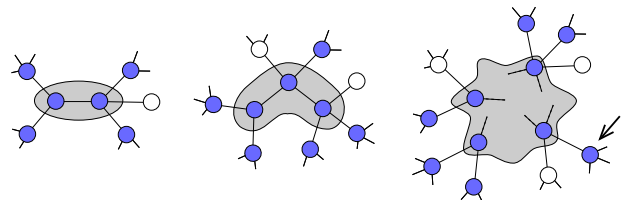


FIG. 4: Corona clusters of different sizes in heterogeneous- $k$ -core. Left: Because they are included unless pruned, two connected vertices (whose threshold is  $k$ ) form part of the heterogeneous- $k$ -core if each has  $k - 1$  other neighbors in the core, as each is 'assisted' by the other. In general (right) a corona cluster consists of vertices (with threshold  $k$ ) that each have exactly  $k$  active neighbors, either inside or outside the cluster. If one neighbor of any of the cluster vertices is removed from the core (for example, the one indicated by the arrow), an avalanche is caused as the entire cluster is pruned.

A subcritical cluster in bootstrap percolation is a cluster of activatable vertices (i.e. not seed vertices) who

each have exactly  $k - 1$  active neighbors external to the cluster. Under the rules of bootstrap percolation, such clusters cannot become activated. The vertices within the cluster block each other from becoming active – see Fig. 3. Now compare the situation for the heterogeneous- $k$ -core. Any cluster of threshold  $k$  vertices which each have  $k - 1$  neighbors in the core external to the cluster, is always included in the heterogeneous- $k$ -core. For the heterogeneous- $k$ -core, vertices in clusters like those in Fig. 4 assist one another. Thus the exclusion of subcritical clusters from activation in bootstrap percolation accounts for the difference in sizes of the bootstrap percolation core and the heterogeneous- $k$ -core.

Subcritical clusters have another important property, that helps us to understand the discontinuity at the second transition. A vertex in a subcritical cluster becomes active if it gains an extra active neighbor (for example through an infinitesimal change in  $p$  or  $f$ ). This in turn allows each of its neighbors in the cluster to activate. A domino-like effect ensues, leading to an avalanche of activations – one extra active neighbor of any vertex in the subcritical cluster leads to the whole cluster becoming active. Thus the rate of change of  $\mathcal{S}_b$  is related to the sizes of the subcritical clusters. Almost everywhere, if we choose a subcritical vertex at random, the mean size of the subcritical cluster to which it belongs is finite. However, exactly at the second threshold, the mean size of the subcritical cluster to which a randomly chosen vertex belongs diverges as we approach from below. This was shown in [41]. Thus, approaching this point, an infinitesimal decrease in  $f$  (or  $p$ ) leads to a finite fraction of the network becoming activated, hence a discontinuity in  $\mathcal{S}_b$  (and also in  $\mathcal{S}_{gc-b}$ ). The distribution of avalanche sizes near the transition is determined by the size distribution  $G(s)$  of subcritical clusters, which at the critical point can be shown to follow  $G(s) \sim s^{-3/2}$ . This can be shown using a generating function approach, as demonstrated in [41]. A similar method can be found in [17, 47–49].

We can then understand the hybrid transition in the heterogeneous- $k$ -core, by considering the relevant clusters with similar properties, the corona clusters. Corona clusters are clusters of vertices with threshold  $k$  that have exactly  $k$  neighbors in the HKC. These clusters are part of the heterogeneous- $k$ -core, but if any member of a cluster loses a neighbor, a domino-like effect leads to an avalanche as the entire cluster is removed from the HKC. The corona clusters are finite everywhere except at the discontinuous transition, where the mean size of corona cluster to which a randomly chosen vertex belongs diverges as we approach from above [6, 17, 47]. Thus, an infinitesimal change in  $f$  (or  $p$ ) leads to a finite fraction of the network being removed from the heterogeneous- $k$ -core, hence a discontinuity in  $\mathcal{S}_k$  (and also in  $\mathcal{S}_{gc-k}$ ). The size distribution of corona clusters, and hence avalanches at this transition also goes as a power law with exponent  $-3/2$ .

### III. SCALE-FREE NETWORKS

The results above, in Sec. I and in Figs. 1 and 2, are qualitatively the same for networks with any degree distribution which has finite second and third moments. When only the second moment is finite, the phase diagram remains qualitatively the same, but the critical behavior is changed. Instead of a second order continuous transition, we have a transition of higher order. When the second moment diverges, we have quite different behavior.

To examine the behavior when the second and third moments diverge, we consider scale-free networks, with degree distributions tending to the form

$$P(q) \approx q^{-\gamma} \quad (6)$$

for large  $q$ . At present we consider only values of  $\gamma > 2$ .

To find the behavior near the critical points, we begin with a self-consistency equation for  $X$ , which is the probability that an arbitrarily chosen edge leads to an infinite  $(k_i - 1)$ -ary tree (see Appendix A). The equation is given in the Appendix, as Eq. (A4). The probability  $\mathcal{S}_{gc-k}$  can be written in terms of  $X$ , and in fact both  $X$  and  $\mathcal{S}_{gc-k}$  grow with the same exponent near the appearance of the giant active component. We expand the right hand side of Eq. (A4) near the appearance of the giant-HKC (that is, near  $X = 0$ ). When  $\gamma < 4$ , the third and possibly second moment of the degree distribution diverge. This means that coefficients of integral powers of  $X$  diverge, and we must instead find leading non-integral powers of  $X$ .

When  $\gamma > 4$ , the second and third moments of the distribution are finite, so the behavior is the same as already described in Sec. I. Eq. (A4) leads to

$$X = c_1 X + c_2 X^2 + \text{higher order terms} , \quad (7)$$

which gives the critical behavior  $X \propto (f - f_{c2-k})^\beta$  with  $\beta = 1$ . When  $3 < \gamma \leq 4$ , the linear term in the expansion of Eq. (A4) survives, but the second leading power is  $\gamma - 2$ :

$$X = c_1 X + c_2 X^{\gamma-2} + \text{higher terms} , \quad (8)$$

where the coefficients  $c_1$  and  $c_2$  depend on the degree distribution, the parameters  $p$  and  $f$ , and the (non-zero) value of  $Z$ . The presence of the linear term means the giant-HKC appears at a finite threshold, but because the second leading power is not 2, the giant-HKC grows not linearly but with exponent  $\beta = 1/(\gamma - 3)$ . This means that the phase diagram remains qualitatively the same as Fig. 2, however, the size of the giant-HKC grows as  $(f - f_{c1})^\beta$  with  $\beta = 1/(\gamma - 3)$ . This is the same scaling as was found for ordinary percolation [50].

For values of  $\gamma$  below 3, the change in behavior is more dramatic. When  $2 < \gamma \leq 3$ , the second moment of  $P(q)$  also diverges, meaning the leading order in the equation for  $X$  is no longer linear but  $\gamma - 2$ :

$$X = d_1 X^{\gamma-2} + \text{higher terms} . \quad (9)$$

From this equation it follows that there is no threshold for the appearance of the giant-HKC (or giant-BPC). The giant-HKC appears immediately and discontinuously for any  $f > 0$  (or  $p > 0$ ), and there is also no upper limit to the threshold  $k$ . This behavior is the same for bootstrap percolation, so the (featureless) phase diagram is the same for both processes, even though the sizes of the giant-HKC and giant-BPC are different.

#### IV. DISCUSSION

We have introduced a new concept, the heterogeneous- $k$ -core, an extension of the well known  $k$ -core of complex networks. A simple representative example of the heterogeneous- $k$ -core (HKC) has vertices with randomly assigned thresholds of either 1 (with probability  $f$ ) or  $k \geq 3$  (with probability  $1 - f$ ). This heterogeneous- $k$ -core has a complex phase diagram, including two types of phase transition: a continuous transition at the appearance of the giant heterogeneous- $k$ -core, similar to the ordinary percolation transition, and a second, discontinuous, hybrid phase transition. This second transition is similar to that found for the ordinary  $k$ -core, but it may occur after the first continuous appearance of the giant-HKC or before. The first transition occurs when the vertices of both kinds reaching their threshold form a giant percolating cluster. The second transition occurs when the mean size of avalanches of pruned vertices diverges. This can be understood by considering corona clusters (clusters of vertices which exactly meet the upper threshold). The mean size of the corona cluster to which an arbitrarily chosen vertex belongs diverges as we approach the second transition from above. The size of pruning avalanches are determined by these corona clusters, and so the transition is discontinuous.

We have contrasted the heterogeneous- $k$ -core with bootstrap percolation, in which there are also two kinds of vertices, but the core is defined by an activation process, rather than a pruning process. The phase diagram for bootstrap percolation therefore does not coincide with that of the heterogeneous- $k$ -core. Furthermore, the two processes can be thought of as two branches of an activation-pruning process, forming a hysteresis loop. The difference between the giant heterogeneous- $k$ -core and the giant bootstrap percolation component results from the subcritical clusters of bootstrap percolation. These clusters cannot be activated as all members have  $k - 1$  active neighbors outside the cluster. However, the equivalent clusters would be included in the giant heterogeneous- $k$ -core.

All of these results are strongly dependent on network structure. If the third moment of the degree distribution is finite, we obtain the results just described, with the giant-HKC growing linearly above the continuous threshold. This is the case if the degree distribution decays faster than a power-law  $q^{-\gamma}$  with  $\gamma > 4$  for large degree  $q$ . If instead the degree distribution tends to a power-law

with  $3 < \gamma \leq 4$ , so that the second moment is finite while the third moment diverges, the phase diagram is qualitatively the same, but the continuous transition is of higher order. If  $2 < \gamma \leq 3$ , the second moment of the degree distribution diverges, and the situation is more extreme. The giant-HKC appears immediately at a finite size for any  $f > 0$  or  $p > 0$ , showing that, in common with behavior found in other systems, such scale-free networks are extremely resilient to damage.

#### Acknowledgments

This work was partially supported by the following projects PTDC: FIS/71551/2006, FIS/108476/2008, SAU-NEU/103904/2008, and MAT/114515/2009, and also by the SOCIALNETS EU project.

#### Appendix A: Self-Consistency Equations

Here we construct the self-consistency equations that the probabilities  $\mathcal{S}_k$ ,  $\mathcal{S}_{gc-k}$ ,  $\mathcal{S}_b$ , and  $\mathcal{S}_{gc-b}$  must obey. The (usually numerical) solution of these equations lead to the phase diagrams and other results presented in Section I. We have already given them for the case of bootstrap percolation [41].

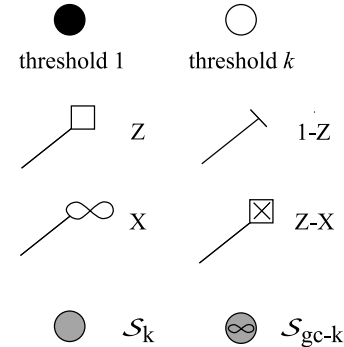


TABLE I: Symbols used in graphical representations of self-consistency equations for the heterogeneous- $k$ -core.

The probability  $\mathcal{S}_k$  that an arbitrarily chosen vertex belongs to the heterogeneous- $k$ -core (HKC) is the sum of the probabilities that it has  $k_i = 1$  and at least one neighbor in the core, or  $k_i = k$  and has at least  $k$  neighbors in the core. We can represent this diagrammatically as:

$$\text{shaded circle} = \text{solid circle} + \left\{ \begin{array}{c} \text{circle with cross} \\ \text{square} \end{array} \right\}_{\geq k}$$

The diagram shows a shaded circle equal to a solid circle plus a set of terms in curly braces with a subscript  $\geq k$ . The terms in the braces are a circle with a cross and a square.

We define  $Z$  in terms of a ' $(k_i - 1)$ -ary tree', a generalization of the  $(k - 1)$ -ary tree. A  $(k_i - 1)$ -ary tree is a sub-tree in which, as we traverse the tree, each vertex

encountered has at least  $k_i - 1$  child edges (edges leading from the vertex, not including the one we entered by). The variable  $k_i$  can be different at each vertex. In our example,  $k_i$  is either 1, in which case the vertex does not need to have any children (though it may have them), and is only required to be connected to the tree, or  $k_i = k$ , in which case it must have at least  $k - 1$  children.

The probability  $Z$  can then be very simply stated as the probability that, on following an arbitrarily chosen edge in the network, we reach a vertex that is a root of a  $(k_i - 1)$ -ary tree. For the specific case considered in this paper, the vertex encountered either has  $k_i = 1$ , or it has  $k - 1$  children leading to the roots of  $(k_i - 1)$ -ary trees. The probability  $Z$  is represented by a square in the diagram. A bar represents the probability  $(1 - Z)$ , a black circle represents a vertex with  $k_i = 1$ , and a white circle a vertex with  $k_i = k$  – see Table I. These conditions can be written as binomial terms, and summing over all possible values of the degree of  $i$ , this diagram can be written in mathematical form as:

$$\mathcal{S}_k = pf \sum_{q=1}^{\infty} P(q) \sum_{l=1}^q \binom{q}{l} Z^l (1 - Z)^{q-l} + p(1 - f) \sum_{q=k}^{\infty} P(q) \sum_{l=k}^q \binom{q}{l} Z^l (1 - Z)^{q-l}, \quad (\text{A1})$$

where the factor  $p$  accounts for the probability that the vertex has not been damaged.

To calculate  $Z$ , we construct a recursive (self consistency) expression in a similar way, based on the definition given above. This is represented by the diagram:

which, in equation form is:

$$Z = pf + p(1 - f) \sum_{q \geq k} \frac{qP(q)}{\langle q \rangle} \sum_{l=k-1}^{q-1} \binom{q-1}{l} Z^l (1 - Z)^{q-1-l} \equiv \Psi(Z, p, f). \quad (\text{A2})$$

We have used that  $qP(q)/\langle q \rangle$  is the probability that the vertex reached along an arbitrary edge has degree  $q$ . Solving Eq. (A2) (usually numerically) for  $Z$  and then substituting into Eq. (A1) allows the calculation of  $\mathcal{S}_k$ .

We follow a similar procedure to calculate the size of the giant heterogeneous- $k$ -core (giant-HKC), which is equal to the probability  $\mathcal{S}_{\text{gc-k}}$  that an arbitrarily chosen vertex is a member of a heterogeneous- $k$ -core component of infinite size. We denote by  $X$  the probability that an arbitrarily chosen edge leads to a vertex which is the root of an infinite  $(k_i - 1)$ -ary tree. That is, the definition is

similar to  $Z$ , but with the extra condition that the subtree reached must extend indefinitely. We represented  $X$  by an infinity symbol (Table I). The diagram for  $\mathcal{S}_{\text{gc-k}}$  is:

which is equivalent to the equation:

$$\mathcal{S}_{\text{gc-k}} = pf \sum_{q=0}^{\infty} P(q) \sum_{m=1}^q \binom{q}{m} X^m (1 - X)^{q-m} + p(1 - f) \sum_{q=k}^{\infty} P(q) \sum_{l=k}^q \binom{q}{l} (1 - Z)^{q-l} \times \sum_{m=1}^l \binom{l}{m} X^m (Z - X)^{l-m}. \quad (\text{A3})$$

To find  $X$ , we construct a self-consistency equation from the diagram

leading to

$$X = pf \sum_{q=0}^{\infty} \frac{qP(q)}{\langle q \rangle} \sum_{m=1}^{q-1} \binom{q-1}{m} X^m (1 - X)^{q-1-m} + p(1 - f) \sum_{q=k}^{\infty} \frac{qP(q)}{\langle q \rangle} \sum_{l=k-1}^{q-1} \binom{q-1}{l} (1 - Z)^{q-1-l} \times \sum_{m=1}^l \binom{l}{m} X^m (Z - X)^{l-m}. \quad (\text{A4})$$

Solution of Eqs. (A2) and (A4) then allows the calculation of  $\mathcal{S}_{\text{gc-k}}$  through Eq. (A3). Note that when there are multiple solutions of  $Z$ , we choose the largest solution as the ‘physical’ one.

To find the appearance of the giant component for a given  $p$ , we find leading terms for  $X \ll 1$ , and solve for  $f$ , as described in Sec. III. To calculate the location of the hybrid transition we note that at this critical point a second solution to Eq. (A2) appears. This occurs when the function  $\Psi(Z)$  just touches the line  $Z$ , which must be at a local extremum of  $\Psi/Z$ :

$$\frac{d}{dZ} \left( \frac{\Psi}{Z} \right) = 0. \quad (\text{A5})$$

Expanding Eq. (A2) about  $Z_c$ , the value of  $Z$  at the critical point (at the top of the jump), and using Eq. (A5),



we see that  $Z$  grows as the square-root of the distance from the critical point. Using Eq. (A1) we find Eq. (3).

Furthermore, at the special point  $p_{s-k}$  where the second transition disappears, by a similar argument, a further condition must also be satisfied:

$$\frac{d^2}{dZ^2} \left( \frac{\Psi}{Z} \right) = 0. \quad (\text{A6})$$

Thus, the critical point  $p_{s-k}$  is determined by simultaneous solution of Eqs. (A2), (A5), and (A6). This in turn leads to cube root scaling above the threshold, hence Eq. (4).

For bootstrap percolation, we can construct similar self-consistency equations in order to calculate  $\mathcal{S}_b$  and  $\mathcal{S}_{\text{gc-b}}$ . Let  $Y$  be the probability (counterpart of  $Z$ ) that on following an arbitrary edge, we encounter a vertex that is either a seed or has  $k$  active children. As discussed in Section II, activation in bootstrap percolation must spread through the network, meaning that the vertex needs  $k$  active downstream neighbors in order to become active (and thus provide an active neighbor to its upstream ‘parent’). Repeating the diagrammatic method described above, we arrive at the equation:

$$Y = pf +$$

$$p(1-f) \sum_{q \geq k+1} \frac{qP(q)}{\langle q \rangle} \sum_{l=k}^{q-1} \binom{q-1}{l} Y^l (1-Y)^{q-1-l} \\ \equiv \Phi(Y, p, f). \quad (\text{A7})$$

Note that Eq. (A7) differs from (A2) because the number of children required is  $k$  not  $k-1$ . This is equivalent to excluding the subcritical clusters represented in Fig. 3. As an aside, consider the probability  $\mathcal{P}_{\text{sub}}$  that an arbitrary edge leads to a vertex in a subcritical cluster. This is clearly simply the probability that the vertex has exactly  $k-1$  active neighbors, thus

$$\mathcal{P}_{\text{sub}} = p(1-f) \sum_{q \geq k} \frac{qP(q)}{\langle q \rangle} \binom{q-1}{k-1} Y^{k-1} (1-Y)^{q-k}. \quad (\text{A8})$$

Comparing Eqs. (A2) and (A7), we see that the right hand side of Eq. (A8) contains precisely the terms that are counted in Eq. (A2) but absent from (A7). Thus clusters of vertices all having exactly  $k-1$  active neighbors are excluded from the active component in bootstrap percolation, while vertices having  $k-1$  neighbors in the heterogeneous- $k$ -core are always included in the heterogeneous- $k$ -core. Of course because of the self-recursion, the value of  $Z$  is necessarily different from that of  $Y$  by more than just the amount of these terms.

Drawing diagrams similar to those given for the heterogeneous- $k$ -core allow the construction of further self-consistency equations for the remaining quantities of interest. The probability that an arbitrarily chosen vertex is active,  $\mathcal{S}_b$  is then identical to Eq. (A1) but with  $Y$

replacing  $Z$ :

$$\mathcal{S}_b = pf \sum_{q=1}^{\infty} P(q) \sum_{l=1}^q \binom{q}{l} Y^l (1-Y)^{q-l} \\ + p(1-f) \sum_{q=k}^{\infty} P(q) \sum_{l=k}^q \binom{q}{l} Y^l (1-Y)^{q-l}. \quad (\text{A9})$$

The equation for  $\mathcal{S}_{\text{gc-b}}$  follows similarly. We introduce the probability  $W$  that, upon following an arbitrary edge, we reach a vertex that is active and also has at least one edge leading to an infinite active subtree. Then  $W$  obeys:

$$W = pf \sum_{q=0}^{\infty} \frac{qP(q)}{\langle q \rangle} \sum_{m=1}^{q-1} \binom{q-1}{m} W^m (1-W)^{q-1-m} \\ + p(1-f) \sum_{q=k+1}^{\infty} \frac{qP(q)}{\langle q \rangle} \sum_{l=k}^{q-1} \binom{q-1}{l} (1-Y)^{q-1-l} \\ \times \sum_{m=1}^l \binom{l}{m} W^m (Y-W)^{l-m}, \quad (\text{A10})$$

which again, differs from Eq. (A4) in that the limit is  $k-1$  not  $k$ . Then  $\mathcal{S}_{\text{gc-b}}$  obeys:

$$\mathcal{S}_{\text{gc-b}} = pf \sum_{q=0}^{\infty} P(q) \sum_{m=1}^q \binom{q}{m} W^m (1-W)^{q-m} \\ + p(1-f) \sum_{q=k}^{\infty} P(q) \sum_{l=k}^q \binom{q}{l} (1-Y)^{q-l} \\ \times \sum_{m=1}^l \binom{l}{m} W^m (Y-W)^{l-m}, \quad (\text{A11})$$

which is identical in form to Eq. (A3), though the values of  $Y$  and  $W$  (for bootstrap percolation) will be different from those of  $Z$  and  $X$  (for the heterogeneous- $k$ -core). Note also that, for bootstrap percolation the physical solution for  $Y$  is always the smallest of Eq. (A7). The discontinuous transition occurs at the point where:

$$\frac{d}{dY} \left( \frac{\Phi}{Y} \right) = 0, \quad (\text{A12})$$

and at the special point  $p_{s-b}$  there is one more condition,

$$\frac{d^2}{dY^2} \left( \frac{\Phi}{Y} \right) = 0, \quad (\text{A13})$$

where the function  $\Phi(Y)$  is defined by Eq. (A7).

Finally we note that the appearance of the giant component of threshold  $k$  vertices in the heterogeneous- $k$ -core process can be found in a similar way to the appearance of the giant-HKC. We define  $R$  to be the probability

that an arbitrarily chosen edge leads to the root of an infinite subtree that is a  $(k_i - 1)$ -ary tree with all of the  $k_i = 1$  vertices removed. This probability then obeys a self consistency equation similar to that for  $X$ :

$$R = p(1 - f) \sum_{q=k}^{\infty} \frac{qP(q)}{\langle q \rangle} \sum_{l=k-1}^{q-1} \binom{q-1}{l} (1 - Z)^{q-1-l} \times \sum_{m=1}^l \binom{l}{m} R^m (Z - R)^{l-m}. \quad (\text{A14})$$

The appearance of the giant component of threshold  $k$  vertices is then found by expanding this equation to leading order with respect to  $R$  and solving for  $f$ . This leads to an equation which gives the dashed line in Fig. 2. Recall that  $Z(f, p)$  is determined by Eq. (A2). A similar procedure yields the corresponding transition in bootstrap percolation.

## Appendix B: General Form of Equations

In this paper, we have examined only a special case of the heterogeneous- $k$ -core, in which vertices have threshold either 1 or  $k \geq 3$ . For completeness, we now give the self-consistency equations for arbitrary threshold distribution  $Q(r)$ . The size  $\mathcal{S}_k$  of the heterogeneous- $k$ -core is

$$\mathcal{S}_k = p \sum_{r \geq 1} Q(r) \sum_{q=r}^{\infty} P(q) \left[ \sum_{l=r}^q \binom{q}{l} Z^l (1 - Z)^{q-l} \right], \quad (\text{B1})$$

where, as above,  $Z$  is the probability of encountering a vertex  $i$  which is the root of a  $(k_i - 1)$ -ary tree:

$$Z = p \sum_{r \geq 1} Q(r) \sum_{q=r}^{\infty} \frac{qP(q)}{\langle q \rangle} \sum_{l=r-1}^{q-1} \binom{q-1}{l} Z^l (1 - Z)^{q-1-l}. \quad (\text{B2})$$

Similarly, the equation for the size of the giant active component is

$$\mathcal{S}_{\text{gc-k}} = p \sum_{r \geq 1} Q(r) \sum_{q=r}^{\infty} P(q) \sum_{l=r}^q \binom{q}{l} (1 - Z)^{q-l} \times \sum_{m=1}^l \binom{l}{m} X^m (Z - X)^{l-m}, \quad (\text{B3})$$

where  $X$  obeys:

$$X = p \sum_{r \geq 1} Q(r) \sum_{q=r}^{\infty} \frac{qP(q)}{\langle q \rangle} \sum_{l=r-1}^{q-1} \binom{q-1}{l} (1 - Z)^{q-1-l} \times \sum_{m=1}^l \binom{l}{m} X^m (Z - X)^{l-m}. \quad (\text{B4})$$

We do not derive any results for this general case, but we can speculate that a more complicated phase diagram would appear. If any vertices have threshold less than 3, i.e.  $Q(1) + Q(2) > 0$ , we would find a continuous appearance of the giant-HKC. Thresholds of 3 or more, on the other hand, contribute discontinuous transitions, and it may be that there are multiple such transitions.

- 
- [1] B. Bollobas, in *Graph Theory and Combinatorics: Proc. of the Cambridge Combinatorial Conf. in honour of Paul Erdos*, edited by B. Bollobas (Academic Press, New York, 1984), pp. 35–37.
  - [2] S. Carmi, S. Havlin, S. Kirkpatrick, Y. Shavitt, and E. Shir, Proceedings of the National Academy of Sciences **104**, 11150 (2007).
  - [3] J. I. Alvarez-Hamelin, L. Dall'Asta, A. Barrat, and A. Vespignani, in *Advances in Neural Information Processing Systems 18*, edited by Y. Weiss, B. Schölkopf, and J. Platt (MIT Press, Cambridge, MA, 2006), pp. 41–50.
  - [4] J. I. Alvarez-Hamelin, L. Dall'Asta, A. Barrat, and A. Vespignani, Networks and Heterogeneous Media **3**, 371 (2008).
  - [5] S. N. Dorogovtsev, A. V. Goltsev, and J. F. F. Mendes, Phys. Rev. Lett. **96**, 040601 (2006).
  - [6] S. N. Dorogovtsev, A. V. Goltsev, and J. F. F. Mendes, Rev. Mod. Phys. **80**, 1275 (2008).
  - [7] C. F. Moukarzel, Phys. Rev. E **68**, 056104 (2003).
  - [8] J. M. Schwarz, A. J. Liu, and L. Q. Chayes, Europhys. Lett. **73**, 560 (2006).
  - [9] N. Chatterjee and S. Sinha, Progr. Brain Res. **168**, 145 (2008).
  - [10] D. J. Schwab, R. F. Bruinsma, J. L. Feldman, and A. J. Levine, Phys. Rev. E **82**, 051911 (2010).
  - [11] P. Klimek, S. Thurner, and R. Hanel, J. Theoret. Biol. **256**, 142 (2009).
  - [12] G. R. Reich and P. L. Leath, J. Stat. Phys. **19**, 611 (1978).
  - [13] J. Chalupa, P. L. Leath, and G. R. Reich, J. Phys. C **12**, L31 (1979).
  - [14] B. Pittel, J. Spencer, and N. Wormald, J. Comb. Theory

- B **67**, 111 (1996).
- [15] D. Fernholz and V. Ramachandran, Tech. Rep. TR04-13, University of Texas Computer Science (2004).
  - [16] M. Molloy, Random Structures Algorithms **27**, 124 (2005).
  - [17] A. V. Goltsev, S. N. Dorogovtsev, and J. F. F. Mendes, Phys. Rev. E **73**, 056101 (2006).
  - [18] O. Riordan, Combin. Probab. Comput. **17**, 111 (2008).
  - [19] B. Corominas-Murtra, J. F. F. Mendes, and R. V. Solé, J. Phys. A **41**, 385003 (2008).
  - [20] F. Sausset, C. Toninelli, G. Biroli, and G. Tarjus, J. Stat. Phys. **138**, 411 (2009).
  - [21] C. L. Farrow, P. Shukla, and P. M. Duxbury, J. Phys. A **40**, F581 (2007).
  - [22] P. Shukla, Pramana journal of physics **71**, 319 (2008).
  - [23] M. Iwata and S. ichi Sasa, J. Phys. A **42**, 075005 (2009).
  - [24] P. M. Kogut and P. L. Leath, J. Phys. C **14**, 3187 (1981).
  - [25] G. Parisi and T. Rizzo, Phys. Rev. E **78**, 022101 (2008).
  - [26] J. P. Gleeson and S. Melnik, Phys. Rev. E **80**, 046121 (2009).
  - [27] J. P. Gleeson, S. Melnik, and A. Hackett, Phys. Rev. E **81**, 066114 (2010).
  - [28] J.-P. Eckmann, O. Feinerman, L. Gruendlinger, E. Moses, J. Soriano, and T. Tlusty, Phys. Rep. **449**, 54 (2007).
  - [29] J. Soriano, M. R. Martínez, T. Tlusty, and E. Moses, Proc. Nat'l Acad. Sci. USA **105**, 13758 (2008).
  - [30] A. V. Goltsev, F. V. de Abreu, S. N. Dorogovtsev, and J. F. F. Mendes, Phys. Rev. E **81**, 061921 (2010).
  - [31] M. Sellitto, G. Biroli, and C. Toninelli, Europhys. Lett. **69**, 496 (2005).
  - [32] C. Toninelli, G. Biroli, and D. S. Fisher, Phys. Rev. Lett. **96**, 035702 (2006).
  - [33] S. Sabhapandit, D. Dhar, and P. Shukla, Phys. Rev. Lett. **88**, 197202 (2002).
  - [34] A. E. Holroyd, Probab. Theory Relat. Fields **125**, 195 (2003).
  - [35] A. E. Holroyd, Electron. J. Probab. **11**, 418 (2006).
  - [36] J. Balogh and B. Bollobas, Probab. Theory Relat. Fields **134**, 624 (2006).
  - [37] R. Cerf and E. N. Cirillo, Ann. Probab. **27**, 1837 (1999).
  - [38] J. Balogh and B. G. Pittel, Random Structures Algorithms **30**, 257 (2007).
  - [39] L. R. G. Fontes and R. H. Schonmann, J. Stat. Phys. **132**, 839 (2008).
  - [40] J. Balogh, Y. Peres, and G. Pete, Combin. Probab. and Comput. **15**, 715 (2006).
  - [41] G. J. Baxter, S. N. Dorogovtsev, A. V. Goltsev, and J. F. F. Mendes, Phys. Rev. E **82**, 011103 (2010).
  - [42] D. E. Whitney (2009), arXiv:0911.4499.
  - [43] D. J. Watts, Proc. Nat'l Acad. Sci. USA **99**, 5766 (2002).
  - [44] J. P. Gleeson, Phys. Rev. E **77**, 046117 (2008).
  - [45] R. Albert and A.-L. Barabási, Rev. Mod. Phys. **74**, 47 (2002).
  - [46] S. N. Dorogovtsev and J. F. F. Mendes, Adv. Phys. **51**, 1079 (2002).
  - [47] S. N. Dorogovtsev, A. V. Goltsev, and J. F. F. Mendes, Physica D **224**, 7 (2006).
  - [48] D. S. Callaway, M. E. J. Newman, S. H. Strogatz, and D. J. Watts, Phys. Rev. Lett. **85**, 5468 (2000).
  - [49] M. E. J. Newman, S. H. Strogatz, and D. J. Watts, Phys. Rev. E **64**, 026118 (2001).
  - [50] R. Cohen, D. ben-Avraham, and S. Havlin, Phys. Rev. E **66**, 036113 (2002).